

# Power Quality improvement in isolated Wind-Diesel Power System

MOHAMED ABDELJABBAR KOUADRIA

Department of Electrical Engineering, Laboratory of Energetic and Computer Engineering  
Ibn Khaldun University, Tiaret 14000, ALGERIA  
abdeldjabbar14@yahoo.fr

TAYEB ALLAOUI

Department of Electrical Engineering, Laboratory of Energetic and Computer Engineering  
Ibn Khaldun University, Tiaret 14000, ALGERIA  
allaoui\_tb@yahoo.fr

MOULOUD DENAI

School of Engineering and Technology  
University of Hertfordshire, Hatfield, UNITED KINGDOM  
m.denai@herts.ac.uk

*Abstract:* - Power quality related disturbances in electrical distribution networks have become a major concern for both network managers and operators associated with the continuous increase of renewable energy resources worldwide. Such disturbances can cause momentary voltage sags and spikes, current distortions and fluctuations in the frequency that directly impact on the efficiency and performance of the electric equipment. This paper proposes a control strategy of a shunt active power filter (SAPF) to enhance the power quality in terms of harmonics and reactive power compensation in a standalone wind-diesel power system. The control of the SAPF is based on the indirect current control (ICC) strategy combining two proportional-integral (PI) controllers with a fuzzy logic controller. The system model is developed under MATLAB/SIMULINK environment and the proposed control scheme is evaluated under varying wind dynamics, linear balanced, unbalanced and non-Linear balanced load conditions.

*Key-Words:* - power quality, wind-diesel, Shunt active power filter, indirect current control, PI, fuzzy logic.

## 1 Introduction

Improved power quality in electrical distribution systems with an increasing penetration of renewable energy resources has become nowadays an important issue for both network managers and for electrical energy operator. Currently, wind energy is among the most viable renewable energy resources in the world, and it is expected that the number and capacity of wind generation installations, in the years ahead, will grow substantially across the world. One of the most promising applications of wind energy is in isolated and remote locations where, usually, wind resources in these areas are fairly high. However, due to the inherent intermittent nature of wind energy and continuously fluctuating wind velocity, a hybrid power system combining a wind energy conversion system with diesel generators has the potential to overcome these limitations.

High penetration for wind-diesel generation is defined as the wind providing at least 75% of the current load for high penetration wind/diesel power

systems without energy storage, there are three operating stage: (1) diesel only, (2) wind/diesel and (3) wind only, the transition between these three separate operating phases is the most challenging part for the power management and control system as both wind and load tend to vary over short time periods.

The operational concept behind these systems is that additional equipment is installed that can insure power system stability and power quality when the diesel engines, the device that typically controls these parameters, is shut down. Major power quality problems which appear are voltage related, frequency variations, harmonics and flickers etc.

Wind diesel hybrid systems have been discussed by many researchers [1-5]. The advantage of this type of hybrid power system is the combination of the continuously available diesel power generation and locally available, pollution-free wind energy. However, the major disadvantage with these sources is that they are generally intermittent or fluctuating in nature. Since the early eighties, the wind diesel

hybrid system have been considered as autonomous electricity generating system using wind turbine generator(s) (WTG) with diesel generator(s) (DG) to obtain a maximum contribution by the intermittent wind resource to the total power produced, while providing continuous high-quality electric power [6]. However, one of the disadvantages is the intermittent nature of wind power generation. Diesel engine driven synchronous generators operating in parallel with wind turbines must maintain a good voltage and frequency regulation against active and reactive load variations and wind speed changes [7-10].

An isolated wind-diesel hybrid system is developed, in which an active shunt power filter is introduced to compensate the harmonics and reactive power of load current demand.

This paper is organised as follows: Sections II and III present a description and mathematical modeling of the hybrid power system respectively. The modelling and control design for the SAPF are presented in Section IV. The model implementation in Matlab/Simulink and simulation results are discussed in Section V. Finally, Section VI summarises the conclusion of the paper.

## 2 Problem Formulation

The proposed system consists of a wind turbine connected to an induction generator, a diesel engine, a synchronous generator, a dumpload, a system load and a shunt active filter (SAPF). A three-phase dumpload is used with each phase consisting of seven transistor-controlled resistor banks. When the wind-generated power is sufficient to serve the load, the diesel engine is disconnected from the synchronous generator by an electromagnetic clutch, and the synchronous generator acts as a synchronous condenser.

A high penetration wind-diesel system has three types of operating conditions: Diesel Only (DO), Wind Diesel (WD) and Wind Only (WO). In DO mode, the maximum power from the wind turbine generator (WTG) is always significantly less than the system load. In this case, the diesel generator (DG) operation never stops and supplies the active and reactive power demanded by the consumer load. But, the DG fuel consumption can be reduced depending on how much power is supplied by the WTG (generally disconnected) and the particular characteristics of the diesel engine.

The synchronous generator (with/without diesel) is used for reactive power control by regulating the terminal voltage via the excitation system. The

synchronous generator also contributes to supply the deficit of reactive power in the induction generator. The SAPF, included in the system for compensating harmonics and reactive power consist of a three phase IGBT-based inverter connected to a DC bus capacitor. The nonlinear load is simulated with a three-phase diode bridge rectifier with R-L load.

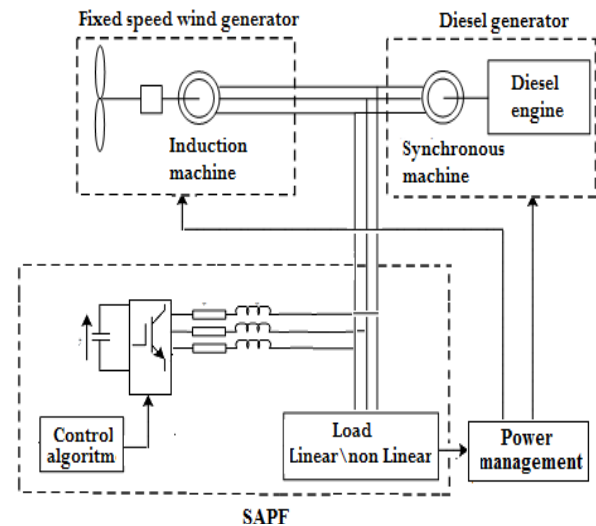


Fig.1 Hybrid system configuration.

## 3 Modeling of the system

### 3.1 Modeling of Wind Power System

The model of a wind energy conversion system (WECS) is based on a horizontal-axis wind turbine connected to an induction generator. The mechanical power ( $P_{tu}$ ) extracted from the wind is mainly governed by three quantities namely, the area swept by rotor blades ( $S$ ), the upstream wind velocity ( $v_0$ ) and the rotor power coefficient ( $C_p$ ) [8, 9].

$$P_{tu} = C_p \times P_{th} = C_p(\lambda, \beta) \frac{\rho \times S \times V_0^3}{2} \quad (1)$$

$C_p$  is a function of the tip speed ratio  $\lambda$  and pitch angle  $\beta$ . The wind turbine considered in this paper is stall-controlled therefore  $\beta$  is constant and  $C_p$  is function of  $\lambda$  only.

$\lambda$  is defined as:

$$\lambda = \frac{\Omega \times R}{V} \quad (2)$$

Where  $\Omega$  is the angular speed of the rotor with radius  $R$ . This function assumes a maximum for a certain value of  $\lambda$ . The operating point of the wind

turbine can be determined from the wind speed input  $V$  and the rotor speed  $\Omega$ . When the induction machine is generating, which corresponds to its operation in the vicinity of synchronous speed, the rotor speed is relatively constant.

The models of the generators are based on the standard Park's transformation that converts all stator variables to a rotor reference frame described by a direct and quadrature (d-q) axis [10].

The electromagnetic torque equation is given by:

$$T_{em} = \frac{3}{2}P(\lambda_{ds} \times i_{qs} - \lambda_{qs} \times i_{ds}) \quad (3)$$

The torque balance equation of mechanical motion of the induction generator side is given as [11, 12]:

$$T_g = J\left(\frac{2}{P}\right)\frac{d\Omega}{dt} + T_{em} \quad (4)$$

Where  $J$  is the inertia,  $P$  is the number poles of the induction generator and  $\Omega$  represents the rotor speed of induction generator.

### 3.1 Modeling of Diesel System

The diesel engine generator is composed of two machines: diesel engine (prime mover) and synchronous generator which models the diesel generator. Using Park's transformation, the electrical quantities like currents, voltages and flux linkages associated with stator and rotor are converted into a two dimensional (d-q) reference frame. The diesel engine unit is developed with standard third order controller and actuator.

The diesel engine model considered here [13-17] consists of a controller to monitor the steady-state speed, a first order actuator with gain  $K$  and time constant  $T_i$  to control the fuel rack position.

Finally, the mechanical torque produced  $T_{mech}$  is represented by the conversion of fuel-flow to torque with a time-delay  $T_D$ .

$$T_{mech}(s) = e^{-sT_D} \Phi(s) \quad (5)$$

Where  $s$  denotes the Laplace transform operator and  $\Phi(s)$  represents the fuel flow.

The diesel engine is a complex device and has many nonlinear components affecting the generation unit performance.

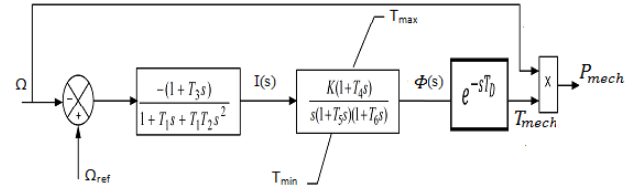


Fig. 2 Model of diesel engine.

## 4 SAPF configuration and control scheme

### 4.1 Overview of SAPF Configuration

Active Power Filters (APFs) are power electronic devices used to suppress harmonics dynamically and provide reactive power compensation. The Shunt APF (SAPF) concept is to use an inverter to produce specific currents or voltages harmonic components to cancel the harmonic components generated by the load. The most common configuration of a SAPF is to inject current harmonics into the point of common coupling (PCC). Fig. 3 shows basic principle of SAPF [18, 19].

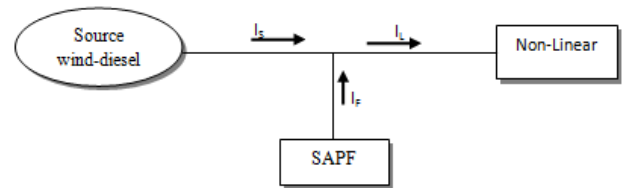


Fig. 3. Basic compensation principle of the SAPF.

With reference to Fig. 3, the source current is given by:

$$i_s(t) = i_L(t) + i_f(t) \quad (6)$$

A voltage source SAPF is supposed to be connected to a balanced three-phase voltage source, with no zero-sequence in the currents.

Applying Kirchhoff's current and voltage laws at the connection point of the SAPF leads to the following equations in the "abc" frame:

$$\begin{cases} V_{sa} = R_f \times i_{fa} + L_f \frac{di_{fa}}{dt} + V_{fa} + V_{MN} \\ V_{sb} = R_f \times i_{fb} + L_f \frac{di_{fb}}{dt} + V_{fb} + V_{MN} \\ V_{sc} = R_f \times i_{fc} + L_f \frac{di_{fc}}{dt} + V_{fc} + V_{MN} \end{cases} \quad (7)$$

The neutral-to-phase SAPF voltages are given by:

$$\begin{cases} V_{f1} = V_{fa} + V_{MN} \\ V_{f2} = V_{fb} + V_{MN} \\ V_{f3} = V_{fc} + V_{MN} \end{cases} \quad (8)$$

Summing the three equations in (8) the ground (M)-to-neutral (N) voltage is given by:

$$V_{MN} = -\frac{1}{3}(V_{fa} + V_{fb} + V_{fc}) \quad (9)$$

By substituting (8) into (9) one can obtain:

$$\begin{cases} V_{f1} = \frac{2}{3}V_{fa} - \frac{1}{3}V_{fb} - \frac{1}{3}V_{fc} \\ V_{f2} = -\frac{1}{3}V_{fa} + \frac{2}{3}V_{fb} - \frac{1}{3}V_{fc} \\ V_{f3} = -\frac{1}{3}V_{fa} - \frac{1}{3}V_{fb} + \frac{2}{3}V_{fc} \end{cases} \quad (10)$$

The equation of DC bus voltage is given by:

$$\frac{dV_{dc}}{dt} = \frac{1}{C}V_{dc} \quad (11)$$

The voltages  $V_{f1}, V_{f2}$  and  $V_{f3}$ , take the values 0 or  $\pm V_{dc}$  depending on the switching function  $C_k$  of the  $k^{th}$  inverter leg ( $k = 1, 2, 3$ ) which is defined as follows:

$$C_k = \begin{cases} 1, \text{ if } s_k \text{ is ON and } s_{k+3} \text{ is OFF} \\ 0, \text{ if } s_k \text{ is OFF and } s_{k+3} \text{ is ON} \end{cases} \quad (12)$$

A switching state function  $d_{nk}$  is defined as:

$$d_{nk} = (C_k - \frac{1}{3} \sum_{m=1}^3 C_m)_n \quad (13)$$

The complete model of the SAPF in the 'abc' frame is:

$$\begin{cases} \frac{di_{fa}}{dt} = -\frac{R}{L_f}i_{fa} - \frac{d_{n1}V_{dc}}{L_f} + \frac{V_{sa}}{L_f} \\ \frac{di_{fb}}{dt} = -\frac{R}{L_f}i_{fb} - \frac{d_{n2}V_{dc}}{L_f} + \frac{V_{sb}}{L_f} \\ \frac{dV_{dc}}{dt} = \frac{1}{C_{dc}}(2d_{n1} + d_{n2})i_{fa} + \frac{1}{C_{dc}}(d_{n1} + 2d_{n2})i_{fb} \end{cases} \quad (14)$$

## 4.2 Control Scheme of the SAPF

There are different methods for generating the current reference for the SAPF in the frequency domain. In this paper, the current reference for the active power filter is generated using the Indirect Control Technique (ICC). Fig. 4 illustrates the ICC scheme. The regulation of dc bus voltage  $V_{dc}$  is very important to ensure effective current control at the input of the SAPF.

Therefore,  $V_{dc}$  should be continuously monitored, conditioned, and compared with a reference value  $V_{dcref}$ . The controller output is multiplied by the phase voltages to get the reference currents  $i_{sa}^*$ ,  $i_{sb}^*$ , and  $i_{sc}^*$ .

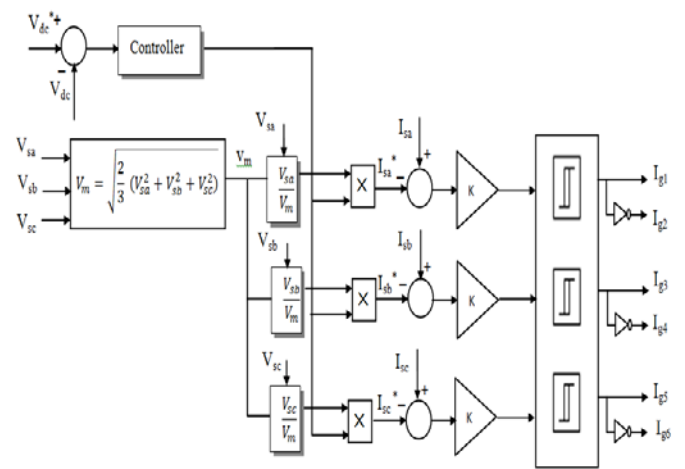


Fig. 4. Indirect current control of the SAPF.

In this technique, the PWM switching signals are obtained by comparing the sensed three-phase supply currents ( $i_{sa}, i_{sb}$  and  $i_{sc}$ ) with their reference counterparts ( $i_{sa}^*, i_{sb}^*$  and  $i_{sc}^*$ ) respectively[18].

$$\begin{aligned} V_{sa} &= V_m \sin(\omega t) \\ V_{sb} &= V_m \sin(\omega t - 120^\circ) \\ V_{sc} &= V_m \sin(\omega t - 240^\circ) \end{aligned} \quad (15)$$

$$u_{sa} = \frac{V_{sa}}{V_m}, \quad u_{sb} = \frac{V_{sb}}{V_m}, \quad u_{sc} = \frac{V_{sc}}{V_m} \quad (16)$$

$$\begin{aligned} i_{sa}^* &= I_{max} \times u_{sa} \\ i_{sb}^* &= I_{max} \times u_{sb} \\ i_{sc}^* &= I_{max} \times u_{sc} \end{aligned} \quad (17)$$

### 4.3 Design Based on PI control

The three phase reference currents (peak value) for the control of the SAPF from the PI controller based on the error between the average dc bus voltage  $V_{dc}$  and its reference value  $V_{dcref}$  of the active filter.

The output of the PI controller has been considered as the amplitude of the desired source current, and the reference currents are estimated as the product of this peak value with the unit sine vectors in phase with the source voltages [10].

The PI-controller of the transfer function is defined as;

$$H(s) = K_p + K_I/s \tag{18}$$

The proportional gain is derived using  $K_p = 2\zeta\omega_{nv}C$ . The damping factor  $\zeta = \sqrt{2}/2$  and natural frequency  $\omega_{nv}$  should be chosen as the fundamental frequency. Similarly, the integral gain is derived using  $K_I = C\omega_{nv}^2$ .

This controller estimates the magnitude of peak reference current  $I_{max}$  and controls the dc-side voltage.

### 4.4 Design Based on Fuzzy Logic Control

Fuzzy systems introduced by Zadeh (1965), have crisp membership functions represented by numbers in [0, 1] and therefore are only able to model vagueness but not uncertainty. Nowadays, fuzzy logic controller (FLC) is used in almost all sectors of industry, power systems and science. The basic schema of fuzzy logic controller is shown in Fig. 5 and consists of four principal components: fuzzification interface which converts input data into suitable linguistic values, a knowledge base which consist of data base with the necessary linguistic definition and control rule set, a fuzzy inference system and a defuzzification interface which yields non fuzzy control action from an inferred fuzzy control action [20, 21].

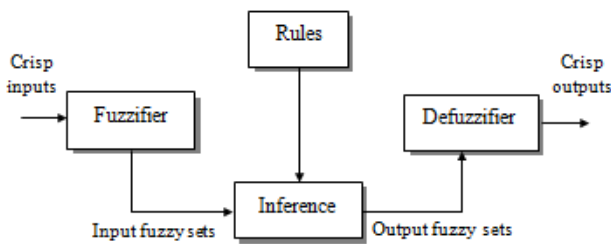


Fig. 5. Standard fuzzy logic system.

In our application, the fuzzy controller acts by processing the voltage error and its variation as shown in Fig. 6.

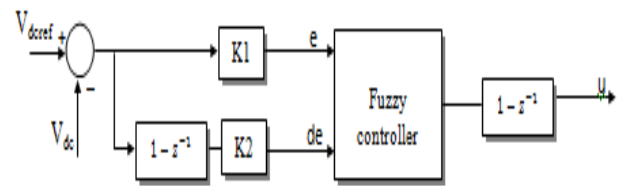


Fig. 6 .DC voltage control using fuzzy control structure.

The fuzzy controller inputs are the error of the DC bus voltage ( $e$ ) and the change of the DC bus voltage error ( $de$ ). These two inputs have three membership functions in linguistic terms. The fuzzy subsets are labelled as N (Negative), EZ (Equal Zero) and P (Positive). The inference method employed here was based on the min-max method and the “centroid” method was used to defuzzify the implied fuzzy control variables.

The membership functions used for the input and output variables are shown in Fig. 7 and the fuzzy rule base is given in the Table 1. The output of the fuzzy controller after a limit is considered as the magnitude of peak reference current  $I_{max}$  Table 1 fuzzy control rules.

TABLE I  
FUZZY CONTROL RULES.

	e		
	N	EZ	P
	de		
N	N	N	EZ
EZ	N	EZ	P
P	EZ	P	P

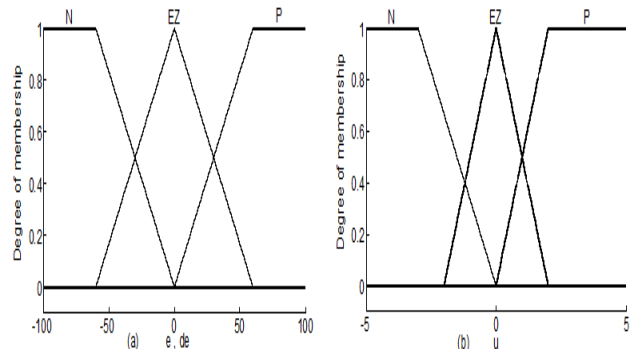


Fig. 7 Membership functions for (a) error, change of error and (b) output (u).

### 5 Simulation and Results

The model parameters used for these simulations are listed in Table 2.

TABLE II  
PARAMETERS OF THE SYSTEM MODEL IN SIMULINK.

System	Values
wind turbine (WT)	$P_n=37\text{kW}$ , $L_s=0.087 \ \Omega$ , $V_n=480\text{V}$ , $R_r'=0.228\Omega$ , $F_r=50\text{Hz}$ , $L_r'=0.8\text{mH}$ , $L_m=34.7\text{mH}$ , $2P=4$ , $R_s=0.087 \ \Omega$ , $J=0.4\text{kg.m}^2$
diesel generator (DG)	$S_n \text{ (kVA)} =37.5$ , $X_{1}' =0.09$ $X_d =3.23$ , $T_{d0} =4.4849$ , $X_d' =0.21$ , $T_{d0}'' =0.0681$ , $X_d'' =0.15$ , $T_{q0}'' =0.1$ , $X_q = 2.79$ , $R_s \text{ (pu)}=0.017$
Consumer load	Main load(kW)=100kW , Nonlinear load $R=35 \ \Omega$ , $L=10^{-3} \ \text{H}$
Active filter	$C=6000 \ \mu\text{F}$ , $L_f=1.8 \ \text{mH}$ $V_{dc}=1200 \ \text{V}$

The overall system has been implemented using Simulink and SimPowerSystems toolboxes as shown in Fig. 8.

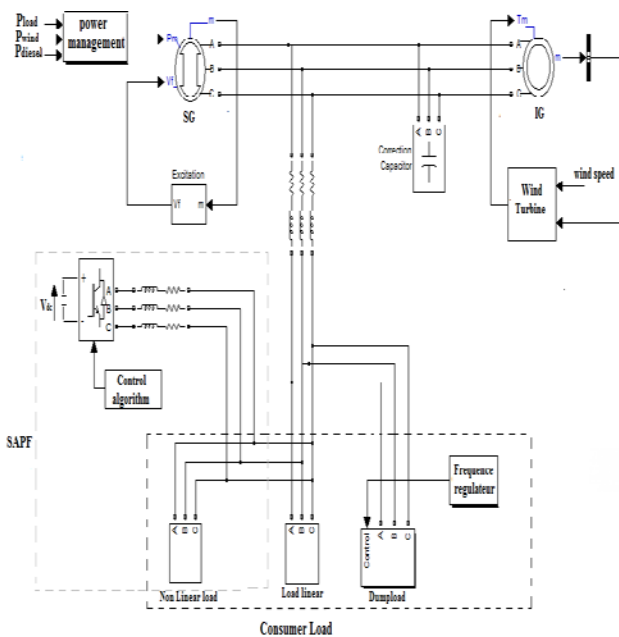


Fig. 8 Simulink model of the system.

To have a constant frequency during all modes of operation, it is necessary that the active power produced by the two sources of energy ( $P_{wind}+P_{diesel}$ ) is equal to that consumed by the  $P_{load}$ .

A series of simulation scenarios have been performed to evaluate the performance of the proposed control methods of the SAPF on the current harmonics under variable load and wind speed conditions.

#### 5.1 Linear Load

Initially, the overall wind-diesel power system is simulated with a linear load variation of 50% applied at  $t = 7 \text{ sec}$  and  $10 \text{ sec}$ . Fig. 9 shows the waveforms of the voltage source ( $v_{sa}$ ), current source ( $i_{sa}$ ), the main load current ( $i_{La}$ ), the secondary load current ( $i_{sa2}$ ) and the system frequency ( $F_r$ ).

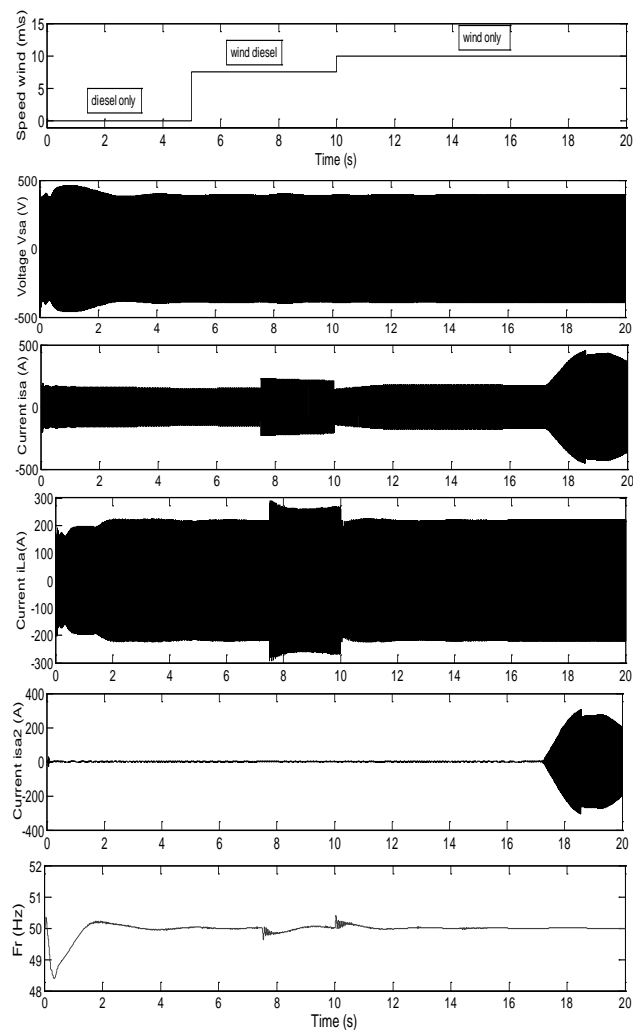


Fig. 9. Wind speed, source voltage, source current, dumpload current, load current and network frequency.

It can be noted that in the case of linear load, the load current remains sinusoidal throughout the simulation time and the voltage and frequency are stable.

**5.2 Nonlinear Load with SAPF and PI controller**

Fig 10 shows the source voltage ( $v_1$ ), source current ( $i_{sa1}$ ), load current ( $i_{ca}$ ), filter current ( $i_1$ ). Fig. 11 and 12 show the DC bus voltage ( $V_{dc}$ ) and harmonic spectrum without and with the SAPF filter respectively.

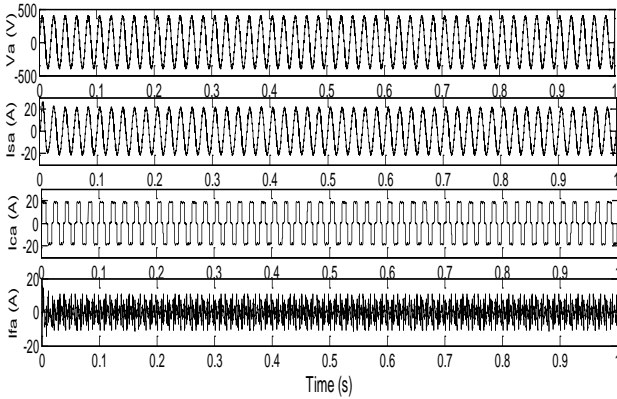


Fig. 10 .Source voltage and source currents, load current and filter current.

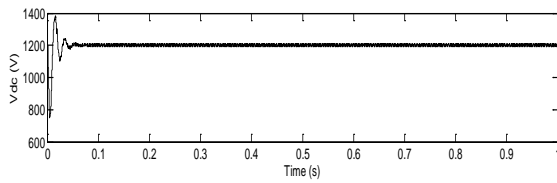


Fig.11. DC bus voltage ( $V_{dc}$ ).

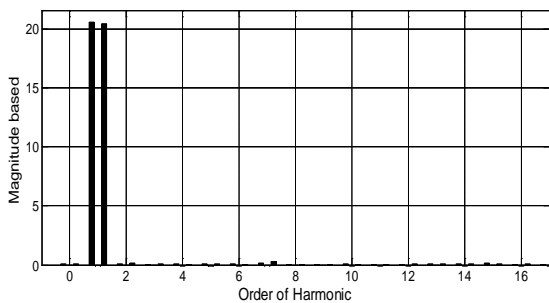
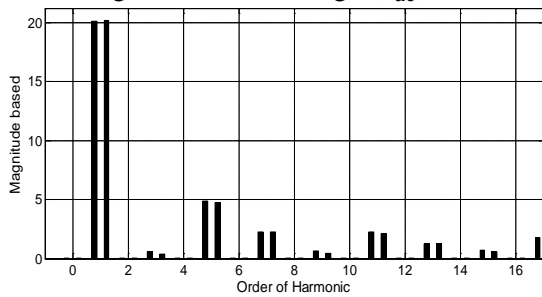


Fig.12 .Total harmonic distortion (THD) spectrum without and with SAPF.

The application of the APF with PI control, has

resulted in a reduction of the THD which dropped from 30.07 % to 2.5 %.

**5.3 Nonlinear Load with SAPF and Fuzzy Controller**

Fig. 13 shows the source voltage ( $v_1$ ), source current ( $i_{sa1}$ ), load current ( $i_{ca}$ ), filter current ( $i_1$ ). Fig. 14 and 15 show the DC bus voltage ( $V_{dc}$ ) and harmonic spectrum without and with the shunt APF filter respectively.

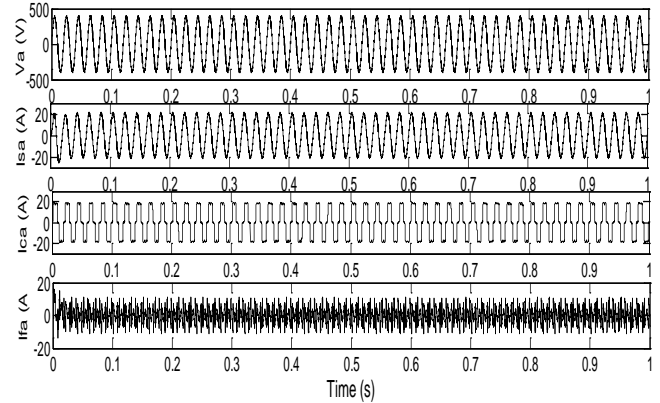


Fig. 13. Source voltage and source currents, load current and filter current.

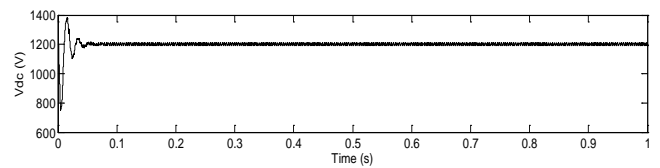


Fig. 14 .DC bus voltage ( $V_{dc}$ ).

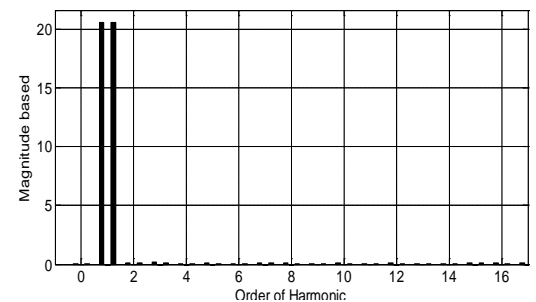
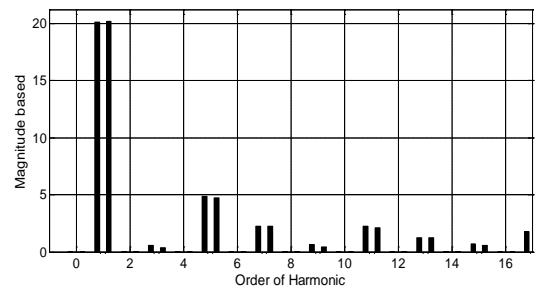


Fig. 15. Total harmonic distortion (THD) spectrum without and with SAPF.

It is clear from simulation results that the transient performance of the source current and DC side capacitor voltage is better with fuzzy logic compared to PI controller. The ability of the SAPF to compensate for the harmonic current of the load filter is demonstrated for the wind-diesel stand-alone system. The results show the effectiveness of the SAPF based on FLC controller. The source current is sinusoidal and in phase with the source voltage. At the harmonic compensation in steady state, the SAPF based on PI controller has a THD about 2.5%. The filter based on FLC leads to a THD of about 0.2%. Both controllers however produce similar transient response performance. Overall, the total harmonic distortion of the current meets the threshold set by the IEEE519 Standard.

A comparison of the three controllers in terms of THD achieved is summarized in Table 3.

TABLE III  
COMPARATIVE PERFORMANCE OF SAPF CONTROLLERS IN TERMS OF THD.

without SAPF		30.07%
with SAPF	PI controller	2.5 %
	Fuzzy controller	2%

## 6 Conclusions

The paper presents a simulation study under Matlab/Simulink of the power management and power quality enhancement strategies for a wind-diesel standalone hybrid power system when connecting a non-linear load. Various control strategies are investigated for the three-phase shunt active power filter (SAPF) to mitigate current harmonics generated by the nonlinear load. The indirect current control strategy was able to suppress the harmonics in the system during balanced sinusoidal, un-balanced sinusoidal and balanced non-sinusoidal conditions.

The simulation studies show that the fuzzy logic controller has resulted in better performance as compared to the PI controller. Finally, the results obtained showed that, with the proposed fuzzy logic-based SAPF controller the supply current is sinusoidal with low harmonic distortion and in phase with the line voltage. The total harmonic distortion of source current has been reduced from a

high value to an allowable limit and to meet the IEEE 519 standard.

### References:

- [1] K. Uhlen, B. A. Foss, O. B. Gjbmter, Robust Control and Analysis of a Wind-Diesel Hybrid Power Plant, IEEE Transactions on Energy Conversion, Vol. 9, No. 4, pp- 701-708, December 1994.
- [2] R. Sebastian, M. Castro, E. Sancristobal, F. Yeves and J. Peire J. Quesada, Approaching hybrid wind-diesel systems and Controller Area Network, IEEE 28th Annual Conference of the Industrial Electronics Society (IECON 02), Vol. 3 , pp- 2300 - 2305, 5-8 Nov. 2002.
- [3] E. Muljadi and H.E. McKenna, Power Quality Issues in a Hybrid Power System, IEEE Transactions on Industry Applications, Vol. 38, No.3, pp.803-809, May/June 2002.
- [4] Hee-Sang Ko, Kwang Y Lee, Min-Jae Kang, Ho-Chan Kim, Power quality control of an autonomous wind-diesel power system based on hybrid intelligent controller, Neural Networks, Vol. 21, No. 10, pp: 1439-1446, 2008
- [5] R. Fadaeinedjad, G. Moschopoulos and M. Moallem, The Impact of Tower Shadow, Yaw Error, and Wind Shears on Power Quality in a Wind-Diesel System, IEEE Transactions on Energy Conversion, Vol. 24, No. 1, pp. 102-111, 2009.
- [6] K. Ghedamsi, D. Aouzellag and EM. Berkouk, Control of wind generator associated to a flywheel energy storage system, Renewable Energy, Vol. 33, No 9, pp: 2145-2156 ,2008.
- [7] Ko .HS, T. Niimura, KY. Lee, An intelligent controller for a remote wind-diesel power system design and dynamic performance analysis, In: Proceedings of IEEE power engineering society general meeting, Vol.4, No 21, pp 47-51, 2003.
- [8] I. Baring-Gould, M. Dabo, Technology, Performance, and Market Report of Wind-Diesel Applications for Remote and Island Communities, Proc. of wind power 2009, Chicago, Illinois . May 4-7, 2009.
- [9] P. Ebert P and J. Zimmermann, Successful high wind penetration into a medium sized diesel grid without energy storage using variable speed wind turbine technology, in Proceedings of EWEC 99, Nice 1999.
- [10] M. Rezkallah, and A. Chandra, Control Of Wind-Diesel Isolated System with Power Quality Improvement, IEEE Electrical Power & Energy Conference (EPEC), 2009.

- [11] A.S. Kini, and R.Y.Udaykumar, Modeling and performance analysis of a wind/diesel hybrid power system, in Proc. IEEE 41th IAS Industry Applications Annual Meeting Conference, Vol. 3 , pp 1215-1221,2006.
- [12] R. Sebastian, Smooth transition from wind only to wind diesel mode in an autonomous wind diesel system with a battery-based energy storage system, Renewable Energy; Vol.33, pp 454-466, 2008.
- [13] G. Iwanski, W. Koczara, Isolated Wind-Diesel Hybrid Variable Speed Power Generation System, presented at EVER 2009, May 26-29, Monaco 2009.
- [14] Bansal RC, Automatic reactive power control of isolated wind-diesel hybrid power systems, IEEE Trans In Electron; Vol.53, No 4, pp 1116-1126 ,2006.
- [15] R. Sebastian, Simulation of the transition from Wind only mode to Wind Diesel mode in a no-storage Wind Diesel System, IEEE Latin American Transactions, IEEE (Revista IEEE America Latina), pp.539-544,Sept. 2009.
- [16] Y. hu, M. McCormick, L. Haydock, M. Cirstea, G.A.Putrus , advance hybrid variable speed controller for stand-alone diesel engine driven generator system, IEEE 2002.
- [17] R.Gagnon, B.Saulnier, G.Sybille, P.Giroux, "Modeling of a generic high-penetration no-storage wind–diesel system using matlab/power system blockset, 2002 Global windpower conference; April 2002.Paris, France.
- [18] B. Singh, A. Chandra, Performance comparison of two current control techniques applied to an active filter, 8th international conference on harmonics and quality of power proceeding, Vol.1 pp 133-8 ,1998.
- [19] S.Rahmani, K.Al-Haddad, , H.Y .Kanaan, Experimental design and simulation of a modified PWM with an indirect current control technique applied to a single-phase shunt active power filter, IEEE International Symposium on Industrial Electronics, vol. 2, pp. 519-524, 2005.
- [20] A. Hamadi, K. EI-Haddad, S. Rahmani, and H. Kankan, Comparison of fuzzy logic and proportional integral controller of voltage source active filter compensating current harmonics and power factor, IEEE International Conference on Industrial Technology (ICIT) , 645-650 ,2004.
- [21] S. Tesnjak, S. Mikus, O. Kuljaca, Load–frequency fuzzy control in power systems, in: Proceedings of the Fifth SONT, Simpozijo Novim Tehnologijima, Poree, 136-139 ,1995.